Finite element-based modal analysis of carbon and glass fiber reinforced column skeletons

ⓘD Ahmet Murat Asan [a,*]

[a] *Dicle University, Department of Mechanical Engineering, Diyarbakir, Turkey.*

ARTICLE INFO

ABSTRACT

Composite materials are used in sectors such as automotive, defense, marine, and aviation due to the high strength and lightness provided by fiber and matrix material. In addition to these sectors, composites are frequently preferred as coating materials in the construction sector to increase the strength of buildings. The basic structure of the building column is formed by concrete, longitudinal reinforcements, and stirrups. Using steel material in longitudinal reinforcements and stirrups is widely preferred in traditional construction applications. However, in this study where the skeleton of a column widely used in the construction sector is designed, Epoxy Carbon Woven Prepreg and Epoxy S-Glass UD composites were used instead of steel in longitudinal reinforcements. The material of the stirrup is steel. Since the skeleton is more flexible than concrete and thus affects the vibration behavior more, concrete modeling as a matrix material was not included in the analysis. Numerical vibration analysis was performed to examine the dynamic behavior of the skeleton. Vibration analysis was performed for both composite materials and steel. As a result of the analysis, the natural frequencies and mode shapes of the structure were determined. In addition, the effect of the use of composites on the vibration results was revealed by comparing the obtained natural frequencies. Using glass fiber composite instead of steel caused a decrease in the average vibration values, while using carbon fiber composite caused an increase. Using carbon and glass fiber caused an increase in deformation.

I. INTRODUCTION

Carbon and glass fiber-reinforced composites have a wide range of industrial uses due to their superior strength and lightness. However, the behavior of fiber-reinforced composite materials under vibration and dynamic loading is an important issue. Therefore, determining and evaluating the vibration properties of fiber-reinforced composites is very important. Vibration tests of fiber-reinforced composites are of critical importance for understanding the mechanical behavior of the material and for material selection in the design process. The main purpose of vibration testing is to determine the resistance of the material to vibration and to provide the information required for vibration prevention design. Vibration tests aim to evaluate the vibration resistance and fatigue life of the material by simulating the conditions under which the material is exposed to vibration. Vibration tests of fiber-reinforced composites are of critical importance for understanding the mechanical behavior of the material and for selecting the right material in the design process. These tests provide the necessary information for the vibration prevention design of the material by determining the vibration resistance and fatigue life of the material. Therefore, the importance and necessity of vibration tests of fiber-reinforced composites should not be ignored. When the studies on natural frequencies of columns used in buildings are examined, Erbaş et al. [1] strengthened concentrically and eccentrically loaded reinforced concrete columns with carbon fiber-reinforced fiber fabric strips. They prepared two of these columns as reference samples and four as strip reinforced. They experimentally investigated the

maximum load-carrying capacity, initial stiffness, ductility, and energy consumption capacity of the six samples they prepared. Ergene [2] investigated the vibration behavior of CFRP composite beams they produced with and without cracks of 1, 2-, 3-, 4-, and 5-mm length using the finite element method (FEM) using the Ansys APDL program. Lyapin and Shatilov [3] investigated the vibration analysis of concrete-reinforced columns experimentally and numerically. Özdemir et al. [4] investigated the effects of steel fiber usage, different boundary conditions, different beam sections, and length parameters on the free vibration behavior of concrete beams experimentally and numerically. The buckling and vibration behavior of stiffened conventional/composite thin-walled box beams was investigated by Ramkumar and Kang [5] using FEM. Pachaiappan [6] investigated the dynamic behavior of a cantilever beam made of functionally graded material (FGM) under free vibration conditions. They used ABAQUS as the finite element program. The vibration characteristics of sandwich beams consisting of an FGM core and functionally graded carbon nanotube reinforced composite (FG-CNTRC) face plates were investigated by Kim and Cho [7] using FEM. With the same method, Belarbi et al. [8] investigated the vibration behavior of symmetric and nonsymmetric functionally graded material sandwich beams (FGSBs) with hard or soft cores using FEM. The frequency response for direct crack detection in an FGM beam was experimentally investigated by Khiem et al. [9]. For this purpose, they used a cracked FGM beam connected by a piezoelectric layer under a moving load. Wang et al. [10] numerically investigated the nonlinear free and forced vibration characteristics of functionally graded graphene-reinforced composite (FG-GPLRC) beams. Ghazwani et al. [11] investigated the nonlinear forced vibration analysis of porous FGM viscoelastic sandwich beams using the numerical method. Jiang and Chen [12] analyzed the vibration and buckling behavior of general composite beams consisting of both transversely laminated and axially bonded materials. For this purpose, they developed and applied a new hybrid FEM. Yan et al. [13] investigated the vibration analysis of variable stiffness composite beams and plates by FEM. Liu et al. [14] numerically determined the free vibration behavior of composite beams and reinforced panels by the FEM method. Davar and Azarafsa [15] determined the natural frequencies of an FGM beam with different boundary conditions. They used FEM as a method. There are also different studies on columns other than vibration analysis [16-25]. The performance of fiber-reinforced polymer (FRP) composite (GPC-FRP) columns having a geopolymer concrete (GPC) matrix subjected to compressive loading was investigated by Veerapandian et al. [16]. Similarly, Wang et al. [17] investigated the compressive behavior of a composite concrete column having an FRP-encased concrete core (EFCCC) by FEM. Sasikumar P. [18] determined the buckling behavior of composite columns made of axially loaded high-strength concrete (HSC) using FEM. The inelastic behavior of pin-ended, axially loaded, concrete-encased steel composite columns was investigated by Ellobody and Young [19]. For this purpose, they developed nonlinear 3D FEM. Prasanna K. and Sandana Socrates S. [20] investigated the performance of concrete-encased steel composite columns under compressive loading. For this purpose, they conducted theoretical and analytical studies. They compared the data obtained with experimental results. Lai et al. [21] investigated the strength behavior of concrete-encased steel composite columns in the case of asymmetric placement using FEM. The load-carrying capacity and energy absorption capacity of increasing the height of the steel profile in concrete-encased steel composite columns were investigated by İnce and Özkal [22] using FEM. Min et al. [23] experimentally investigated the behavior of recycled aggregate concrete (RAC)-encased recycled aggregate concrete-filled steel tube (RACFST) composite columns under axial compressive loading. CFRP (carbon fiber reinforced polymer)-reinforced timber columns were produced by Siha and Zhou [24]. They experimentally and numerically investigated the behavior of the columns they produced under lateral

cyclic loading. They used FEM in their numerical studies. Sun et al. [25] investigated the flexural behavior of steel fiber reinforced beams strengthened with glass fiber reinforced polymer (GFRP) rods using FEM.

When the literature is examined, it is seen that the studies have made rectangular [1-25] or circular [26-28] flat column designs, but the reinforcement and stirrups are not included in the numerical designs [2-8, 10-28]. However, the steel used in the skeleton of the column is more flexible than the concrete. In this way, the skeleton affects the vibration behavior more than the concrete, and it is important to examine it individually. Because in cases where the concrete, which is the matrix element, has lost its properties, the skeleton must withstand vibration-effective situations such as earthquakes on its own. This study aims to answer the question of how the use of CFRP or GFRP composite instead of steel, which is mostly used in longitudinal reinforcement, will affect the vibration behavior and deformation results of the column skeleton. In the experimental study conducted for columns [1], the use of CFRP and in the numerical study [5], the use of GFRP and CFRP was effective in selecting CFRP and GFRP as parameters. For this purpose, the vibration analysis of the column skeleton created by designing longitudinal reinforcement and stirrups was performed numerically.

II. MATERIALS AND METHODS

Within the scope of the numerical study, the experimental elements whose dimensions are shown in Figure 1 were designed. Literature [1, 29] was used in the creation of the dimensions used in the designs. The models were prepared in the CAD program and converted to the ".step" format. Then, they were transferred to ANSYS Workbench. Steel, CFRP composite and GFRP composite were used as the longitudinal reinforcement material selected with a diameter of 10 mm. The material of the 4 mm diameter stirrup designed as 20 pieces was steel. The mechanical properties of the materials used are given in Table 1. These properties were taken from the ANSYS Workbench library [30, 31]. In order to avoid any calculation errors, the mechanical properties used were compared with the values in the literature. It was determined that the values used for CFRP [32, 33], GFRP [34, 35], and structural steel [36] were similar.

Table 1. Mechanical properties of materials [30, 31]

Material	E_x (MPa)	E_y (MPa)	E_z (MPa)	v_{xy}	v_{yz}	v_{xz}	G_{xy} (MPa)	G_{yz} (MPa)	G_{zx} (MPa)	Density (kg/mm³)
CFRP	91820	91820	9000	0.05	0.3	0.3	3600	3000	3000	1.48×10^{-6}
GFRP	50000	8000	8000	0.3	0.4	0.3	5000	3846.2	5000	2×10^{-6}
Structural Steel	200000	-	-	0.3	-	-	-	-	-	7.85×10^{-6}

In Table 1, E_x, E_y, and E_z represent the elasticity modules in the x, y and z directions; v_{xy} represents the Poisson ratio for the $x - y$ plane; v_{yz} represents the Poisson ratio for the $y - z$ plane; v_{xz} represents the Poisson ratio for the $x - z$ plane; G_{xy} represents the shear module in the $x - y$ plane; G_{yz} represents the shear module in the $y - z$ plane; G_{xz} represents the shear module in the $x - z$.

The finite element model of the designed test elements, the boundary conditions applied to the model, and the number of elements and nodes of this model are given in Table 2. Four reinforcements were fixed from the bottom as a boundary condition. Bonded contact type was used to ensure that the longitudinal reinforcement and stirrups move together. Sevim and Altunışık [37] determined the vibration analysis of composite columns with different cross-sections with FEM. It was observed that the number of elements and nodes in the models they used was

lower than those in Table 2. The boundary condition is the same. Because free vibration analysis was also performed in the study. For this reason, the model was fixed at one end. A mesh convergence study was performed to obtain the optimum values (Figure 2). In the mesh convergence graph, when it was observed that the deformation value remained constant with the increase in the number of nodes, it was decided that it would be appropriate to use the mesh size value.
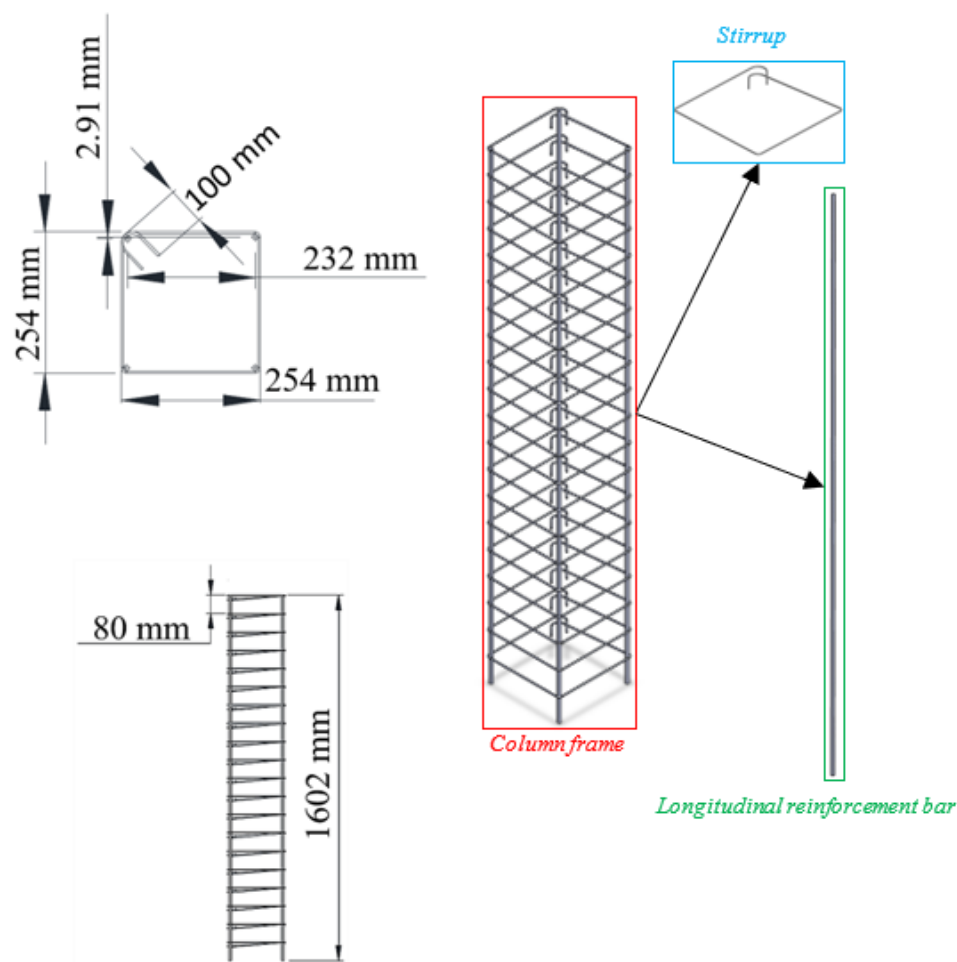

Table 2. Finite element model of the designed test elements, boundary conditions applied to the model, number of elements, and number of nodes belong to this model

Finite Element Model with Boundary Conditions	$u_x = u_y = u_z = 0$
Number of Elements	34736
Number of Nodes	78223
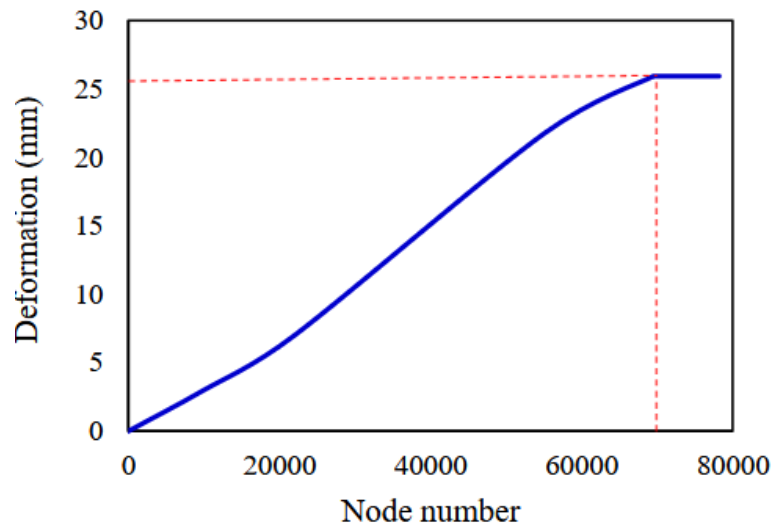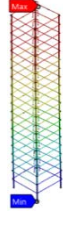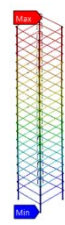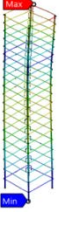
Figure 2. Mesh convergence analysis

III. RESULTS AND DISCUSSION

The frequency deformation table for the six modes obtained because of the vibration test of the samples is given in Table 3. This table also shows the percentage change rates of frequency and deformation changes according to Mode 1. In order to better understand the changes in frequencies and deformations, the changes in frequencies and deformations according to modes are given in Figure 3. According to Figure 3a, frequencies increase according to the number of modes. While the frequency transition between Mode 1-Mode 2 and Mode 3-Mode 4 is close to flat for all materials, a line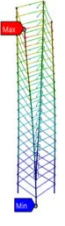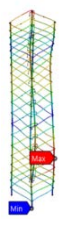ar increase is observed between Mode 2-Mode 3 and Mode 5-Mode 6. The frequency change shown by steel between Mode 3-Mode 5 remained low compared to GFRP and CFRP. The rigidity of steel remained almost constant in these modes. Because the response of steel to bending and torsion modes is lower than that of FRP materials. Since FRP materials are linear-elastic and brittle by their nature, they showed sharper frequency increases compared to steel, which is a ductile material. The curve is linear between Mode 5 and Mode 6 for all of them. When Figure 3b is examined, it is seen that the change between Mode 1 and Mode 2 is like Figure 3a. The deformation increases between Mode 2-Mode 3 increased depending on the frequency increase. However, the behavior of steel between Mode 3-Mode 5 was different from FRP materials. Steel showed a decrease despite the frequency change remaining almost constant between Mode 3-Mode 4. In this case, the structure was less stressed, so the deformation decreased. In the similar case between Mode 4-Mode 5, it increased. Because the cracks or material weakening in the structure reduced the rigidity. When the data in Table 3 is examined, it is seen that the highest frequency occurs in Mode 6 in all three reinforcement materials. This situation is due to the fact that the smallest frequency obtained because of the ordering of natural frequencies from smallest to largest is called the fundamental frequency, and the mode shape corresponding to this frequency is called the first mode shape [5-7, 9, 38, 39]. It was observed that the smallest natural frequencies are generally seen in GFRP, but they suddenly increase in Mode 5 due to fiber breakage. Toptaş E. et al. investigated the strength losses caused by fiber breakage in unidirectional cantilever beam composites in FRP composites by vibration analysis method. They stated that the breakage of the fibers will reduce the strength [40]. Naya et al. [41] also reported the same effect. The largest natural frequencies were seen in CFRP. This situation is a result of high brittleness [42]. Kroisová et al. They

FEM modal analysis

J. Innovative Eng. Nat. Sci. vol. 5, no.2, pp. 652-662, 2025.

performed fiber destruction in CFRP and GFRP composites. For this purpose, they applied milling, drilling, and grinding to the composites. As a result, they stated that CFRP breaks with hard fracture and GFRP breaks with brittle fracture due to their nature [43]. The highest deformation for steel was observed in Mode 3, while it occurred in Mode 5 for GFRP and CFRP.

Table 3. Frequency-deformation table

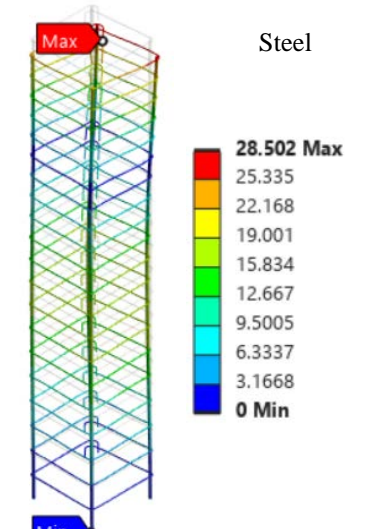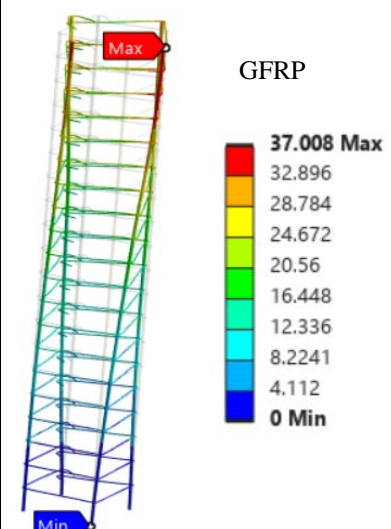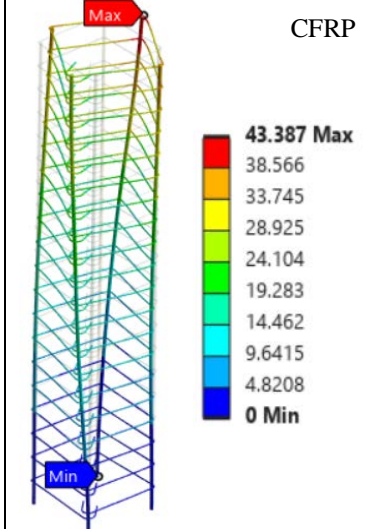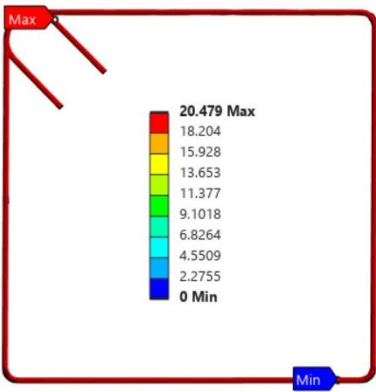| Mode	Frequency (Hz)			Deformation (mm)			Deformation Shapes		
	Steel	GFRP	CFRP	Steel	GFRP	CFRP	Steel	GFRP	CFRP
1	9.2568	7.6659	9.7106	20.479	25.942	28.717			
%difference	-	-	-	-	-	-			
2	10.047	8.3521	10.737	20.515	26.592	29.083			
%difference	+8.54	+8.95	+10.57	+0.18	+2.51	+1.27			
3	28.894	22.716	30.112	28.502	31.020	38.097			
%difference	+212.14	+196.33	+210.09	+39.18	+19.57	+32.66			
4	29.667	24.037	31.902	23.982	33.457	40.158			
%difference	+220.49	+213.56	+228.53	+17.11	+28.97	+39.84			
5	30.462	31.010	34.757	28.105	37.008	43.387			
%difference	+229.08	+304.52	+257.93	+37.24	+42.66	+51.08			
6	38.598	38.634	49.774	25.375	31.077	38.287			
%difference	+316.97	+403.97	+412.57	+23.91	+19.79	+33.33			
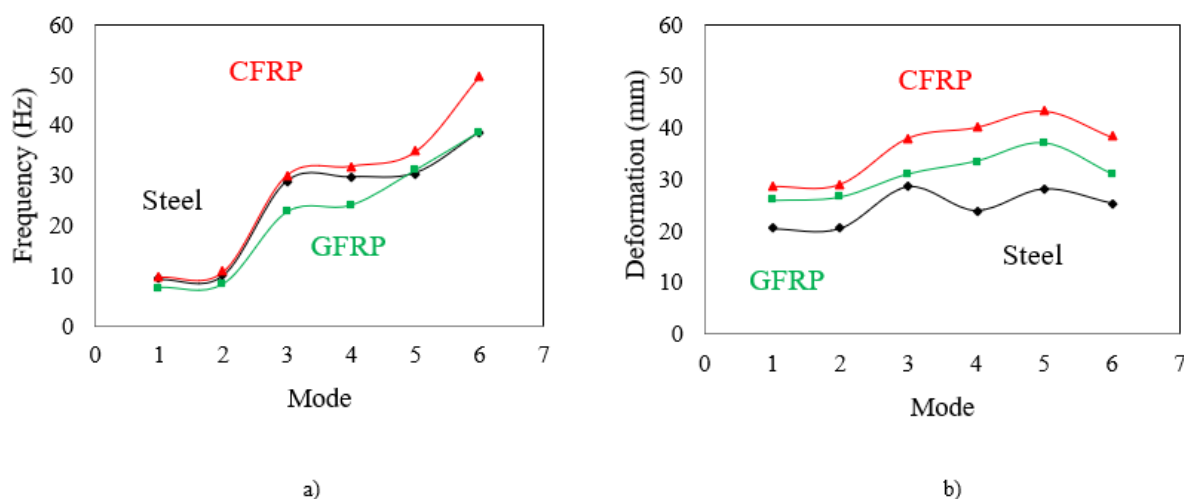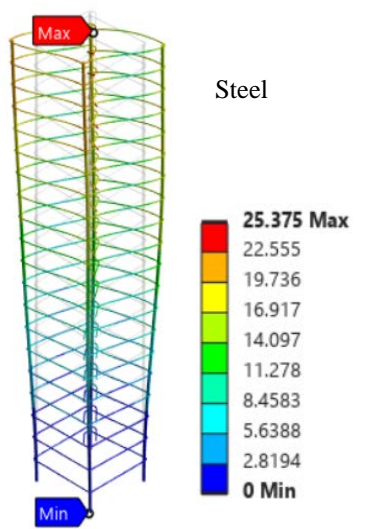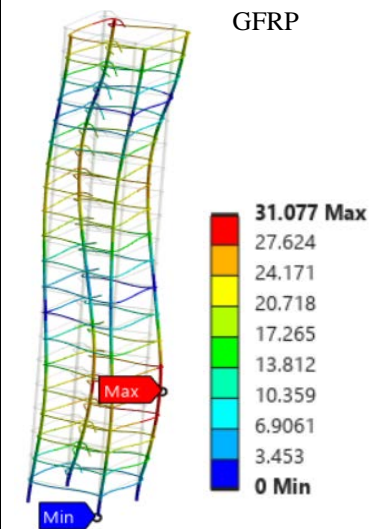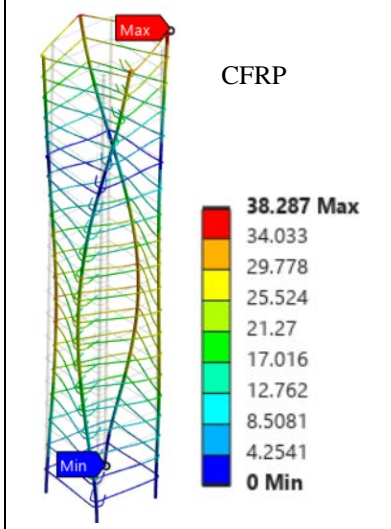
Figure 3. Changes in frequency and deformations according to modes a) Frequency-mode graph, b) Deformation-mode graph
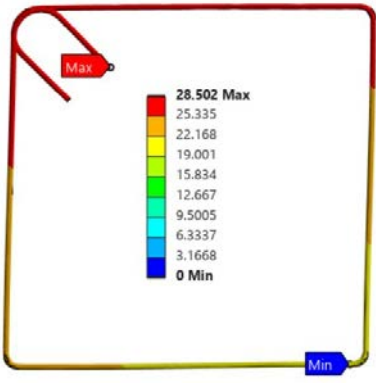
In Table 4, the results of the modes in which the highest frequencies and deformations were detected are given separately. According to these results, the minimum deformations were in the section where the skeleton was fixed, while the maximum deformations were seen at the free end. The place where the maximum frequency was seen was in the same section for steel and CFRP, while it was in the lower section for GFRP. The place where the minimum frequency was seen was the same for steel, GFRP, and CFRP. It is seen from the deformation patterns that this situation is caused by the torsion in Mode 5. When passing from Mode 5, where the fibers are broken, to Mode 6, a recovery in the structure of the fibers caused a decrease in frequency. In the case of steel, in Mode 3, the uppermost stirrup was exposed to the highest vibration singularly. Therefore, the stirrup structure opened, allowing the highest deformation to be seen within its own values. In order to see this situation more clearly, the change of the highest deformation mode shown by the steel stirrup compared to Mode 1 is given in Figure 4. While the stirrup has a square shape in Mode 1, it is seen that it opens and takes a parallelogram shape in Mode 3. When the percentage changes are examined, it is determined that the deformation increase in steel starts quite low (0.18%) but then increases and shows more deformation than GFRP in Mode 6. For Mode 2, the increase was higher in GFRP and CFRP, unlike steel. This situation shows that the response of steel to bending modes is less than that of GFRP and CFRP. The same response situations were repeated in torsion modes. The percentage changes in deformation were low compared to the percentage changes in frequency. The different behaviors of FRP and steel materials are mainly due to the fact that steel is isotropic and FRP materials are anisotropic, and the elasticity modulus and density of steel materials are different from those of FRP materials. In addition, the densities of the materials used in the study have an important effect on the results. Because natural frequency is a frequency that depends on stiffness and mass.

Table 4. Results for the modes in which the highest frequencies and deformations were detected

Modes in which the highest frequencies are detected		
Steel	GFRP	CFRP
25.375 Max 22.555 19.736 16.917 14.097 11.278 8.4583 5.6388 2.8194 0 Min	31.077 Max 27.624 24.171 20.718 17.265 13.812 10.359 6.9061 3.453 0 Min	38.287 Max 34.033 29.778 25.524 21.27 17.016 12.762 8.5081 4.2541 0 Min
Mode 6	Mode 6	Mode 6
Modes in which the highest deformations were detected		
Steel	GFRP	CFRP
28.502 Max 25.335 22.168 19.001 15.834 12.667 9.5005 6.3337 3.1668 0 Min	37.008 Max 32.896 28.784 24.672 20.56 16.448 12.336 8.2241 4.112 0 Min	43.387 Max 38.566 33.745 28.925 24.104 19.283 14.462 9.6415 4.8208 0 Min
Mode 3	Mode 5	Mode 5

a)

20.479 Max
18.204
15.928
13.653
11.377
9.1018
6.8264
4.5509
2.2755
0 Min

b)

28.502 Max
25.335
22.168
19.001
15.834
12.667
9.5005
6.3337
3.1668
0 Min

Figure 4. The highest deformation shown by the steel stirrup; a) Mode 1, b) Mode 3

IV. CONCLUSIONS

In a structure consisting only of reinforcement and stirrups, the effect of selecting CFRP and GFRP as reinforcement material in addition to steel on natural frequency and deformation status was examined, and certain results were reached. These are;

• As the number of modes increases, the natural frequency values of the structure increase.

• The material that showed the highest deformation was CFRP.

• While the highest deformation in steel material was observed in Mode 3 (+39.18), it was detected in Mode 5 in GFRP (+42.66) and CFRP (+51.08) materials.

• It was understood that the use of CFRP caused an increase in vibration. In Mode 6, the increase is 412.57% compared to the first case. This increase is 95.6% more than that of steel and 8.6% more than that of GFRP for the same mode.

• The use of GFRP as reinforcement material provided an average of lower vibration values.

• The use of CFRP and GFRP caused high deformations in the structure.

• Bending modes were seen in the modes before torsional modes. This situation is preferable because torsional modes can cause significant damage to structures.

• The response of FRP materials in bending and torsion modes is more sensitive than that of steel.

The models examined within the scope of this study were evaluated according to the selected material properties, element dimensions and mesh quality. Therefore, in order to provide more general information on this subject, analyses can be made for materials with different mechanical properties. In future studies, concrete can be included in the modeling and the vibration behavior it will exhibit with the skeleton can be examined. Experimental studies can also be conducted and the results can be compared.

REFERENCES

1. Erbaş Y, Baran M, Mercimek Ö, Anıl O (2022) Karbon fiber takviyeli elyaf kumaşlarla güçlendirilen betonarme kolonların eş merkezli ve tek doğrultulu eğilme yüklemeleri altındaki davranışının deneysel olarak incelenmesi. Bayburt Univ Fen Bilim Derg 5(1):91–103. https://doi.org/10.55117/BUFBD.1118830
2. Ergene B (2021) Çatlak derinliğinin ve fiber açısının karbon fiber takviyeli polimer kompozit kirişin titreşim davranışına etkisinin sonlu elemanlar analizi yöntemi ile belirlenmesi. Int J 3D Print Technol Digit Ind 5(2):120–129. https://doi.org/10.46519/IJ3DPTDI.931530
3. Lyapin A, Shatilov Y (2016) Vibration-based damage detection of the reinforced concrete column. Procedia Eng 150:1867–1871. https://doi.org/10.1016/j.proeng.2016.07.184
4. Özdemir MT, Kobya V, Yaylı MÖ, Mardani-Aghabaglou A (2021) Vibration analysis of steel fiber reinforced self-compacting concrete beam on elastic foundation. Comput Concr 27(2):85–97. https://doi.org/10.12989/CAC.2021.27.2.085
5. Ramkumar K, Kang H (2013) Finite element based investigation of buckling and vibration behaviour of thin walled box beams. Appl Comput Mech 7(2):155-182.
6. Pachaiappan S (2024) Free vibration analysis of FGM beam by numerical analysis. Innov Infrastruct Solut 9(8). https://doi.org/10.1007/s41062-024-01647-7
7. Kim HJ, Cho J (2024) Numerical free vibration analysis of sandwich beams with a steel-ceramic FGM core and FG-CNTRC facesheets. Int J Steel Struct 24(4):734–742. https://doi.org/10.1007/s13296-024-00858-z
8. Belarbi M, Khechai A, Houari MSA, Bessaim A, Hirane H, Garg A (2024) Free vibration behavior of sandwich FGM beams: Parametric and uncertainty analysis. J Vib Eng Technol. https://doi.org/10.1007/s42417-024-01452-7
9. Khiem NT, Huan DT, Hieu TT (2022) Vibration of cracked FGM beam with piezoelectric layer under moving load. J Vib Eng Technol 11(2):755–769. https://doi.org/10.1007/s42417-022-00607-8
10. Wang R, Zhong R, Wang Q (2024) A SGM-IHB approach for nonlinear free and forced vibration analysis of FG-GPLRC beams rested on viscoelastic foundation. Nonlinear Dyn. https://doi.org/10.1007/s11071-024-

10506-0

11. Ghazwani MH, Alnujaie A, Youzera H, Meftah SA, Tounsi A (2024) Nonlinear forced vibration investigation of the sandwich porous FGM beams with viscoelastic core layer. Acta Mech 235(5):2889–2904. https://doi.org/10.1007/s00707-024-03865-7

12. Jiang J, Chen W (2024) Dynamic behaviors of general composite beams using mixed finite elements. Int J Mech Sci 281:109687. https://doi.org/10.1016/j.ijmecsci.2024.109687

13. Yan Y, Liu B, Xing Y, Carrera E, Pagani A (2021) Free vibration analysis of variable stiffness composite laminated beams and plates by novel hierarchical differential quadrature finite elements. Compos Struct 274:114364. https://doi.org/10.1016/j.compstruct.2021.114364

14. Liu X, Pagani A, Carrera E, Liu X (2024) Free vibration analysis of composite beams and laminated reinforced panels by refined dynamic stiffness method and CUF-based component-wise theory. Compos Struct 337:118058. https://doi.org/10.1016/j.compstruct.2024.118058

15. Davar A, Azarafza R (2023) Free vibration analysis of functionally graded annular circular plates using classical thin plate theory based on physical neutral surface. J Vib Eng Technol 12(3):3873–3896. https://doi.org/10.1007/s42417-023-01092-3

16. Veerapandian V, Pandulu G, Jayaseelan R, Kumar VS, Murali G, Vatin NI (2022) Numerical modelling of geopolymer concrete in-filled fibre-reinforced polymer composite columns subjected to axial compression loading. Materials 15(9):3390. https://doi.org/10.3390/ma15093390

17. Wang X, Qi Y, Sun Y, Xie Z, Liu W (2019) Compressive behavior of composite concrete columns with encased FRP confined concrete cores. Sensors 19(8):1792. https://doi.org/10.3390/s19081792

18. Sasikumar P (2023) A comparative study between buckling behaviour and statistical analysis of axially loaded fully encased composite columns made with high strength concrete. Rev Constr 22(3):694–706. https://doi.org/10.7764/rdlc.22.3.694

19. Ellobody E, Young B (2010) Numerical simulation of concrete encased steel composite columns. J Constr Steel Res 67(2):211–222. https://doi.org/10.1016/j.jcsr.2010.08.003

20. Prasanna K, Sandana Socrates S (n.d.) Study on the structural behavior of concrete encased steel composite column. Int Res J Eng Technol 6:4254-4259.

21. Liew JYR, Lai B, Li S (2018) Finite element analysis of concrete-encased steel composite columns with off-center steel section.12th Int Conf Advances in Steel-Concrete Composite Struct. València, Spain, Jun. 27-29. https://doi.org/10.4995/asccs2018.2018.7005

22. İnce EG, Özkal FM (2024) Optimization of structural steel used in concrete-encased steel composite columns via topology optimization. Appl Sci 14(3):1170. https://doi.org/10.3390/app14031170

23. Cai M, Ke X, Su Y (2020) Axial compressive performance of RAC-encased RACFST composite columns. Eng Struct 210:110393. https://doi.org/10.1016/j.engstruct.2020.110393

24. Siha A, Zhou C (2023) Experimental study and numerical analysis of composite strengthened timber columns under lateral cyclic loading. J Build Eng 67:106077. https://doi.org/10.1016/j.jobe.2023.106077

25. Sun Y, Liu Y, Wu T, Liu X, Lu H (2019) Numerical analysis on flexural behavior of steel fiber-reinforced LWAC beams reinforced with GFRP bars. Appl Sci 9(23):5128. https://doi.org/10.3390/app9235128

26. Shen Z, Liu B, Zhou G (2022) Stressing state analysis of SRC column with modeling test and finite element model data. Appl Sci 12(17):8866. https://doi.org/10.3390/app12178866

27. Zhou X, Liu J (2010) Seismic behavior and strength of tubed steel reinforced concrete (SRC) short columns. J Constr Steel Res 66(7):885–896. https://doi.org/10.1016/j.jcsr.2010.01.020

28. Zhu Y, Wang W, Shi Y, Li M, Wang S, Bao L, Tian Y (2023) Experimental and numerical study on seismic behavior of partially steel-reinforced concrete beam-to-steel tube column joint. J Build Eng 76:107210. https://doi.org/10.1016/j.jobe.2023.107210

29. Engineering Discoveries (2025) Information about reinforcement of columns. https://engineeringdiscoveries.com/information-about-reinforcement-of-columns. Accessed 25 Jun 2025

30. ANSYS (2024) GRANTA Materials Data for Simulation (Sample). https://www.ansys.com/products/materials. Accessed 9 Oct 2024

31. ANSYS (2021) Material property data for engineering materials. https://www.ansys.com/content/dam/amp/2021/august/webpage-requests/education-resources-dam-upload-batch-2/material-property-data-for-eng-materials-BOKENGEN21.pdf. Accessed 25 Jun 2025

32. Riccio A, Saputo S, Sellitto A, Russo A, Di Caprio F, Di Palma L (2019) An insight on the crashworthiness behavior of a full-scale composite fuselage section at different impact angles. Aerospace 6(6):72. https://doi.org/10.3390/aerospace6060072

33. Zhou R, Gao W, Liu W (2021) An MMF3 criterion based multi-scale strategy for the failure analysis of plain-woven fabric composites and its validation in the open-hole compression tests. Materials 14(16):4393. https://doi.org/10.3390/ma14164393

34. El-Nemr A, Ashour O, Hekal G (2016) Finite element modeling of confined concrete piles with FRP tubes in sandy soil under static loading. In: CRC Press eBooks, pp 2122–2127.

https://doi.org/10.1201/9781315641645-351

35. Bhatnagar N, Nayak D, Singh I, Chouhan H, Mahajan P (2004) Determination of machining-induced damage characteristics of fiber reinforced plastic composite laminates. Mater Manuf Process 19(6):1009–1023. https://doi.org/10.1081/amp-200035177

36. Liu Y (2013) Choose the best element size to yield accurate FEA results while reduce FE model's complexity. Br J Eng Technol 1(7):13-28.

37. Sevim B, Altunişik AC (2017) Kompozit kolon elemanların modal davranışlarının belirlenmesi. DÜMF Müh Derg 8(1):13–24. https://doi.org/10.24012/dumf.386614

38. Petyt M (1990) Introduction to finite element vibration analysis. Cambridge University Press, Cambridge

39. Chopra AK (2006) Dynamics of structures: Theory and applications to earthquake engineering, 3rd edn. Prentice Hall, USA

40. Toptaş E, Ersoy S, Bozkurt Y (2018) Investigation on vibration analysis of the effect of fiber breaks in unidirectional composites. Online J. Sci. Technol. 8(3):74-79.

41. Naya F, Pernas-Sánchez J, Fernández C, Zumel P, Droździel-Jurkiewicz M, Bieniaś J (2024) Experimental study of the importance of fibre breakage on the strength of thermoplastic matrix composites subjected to compression after impact. Compos Struct 342:118238. https://doi.org/10.1016/j.compstruct.2024.118238

42. Pramanik A, Basak A, Dong Y, Sarker P, Uddin M, Littlefair G, Dixit A, Chattopadhyaya S (2017) Joining of carbon fibre reinforced polymer (CFRP) composites and aluminium alloys – A review. Compos Part A Appl Sci Manuf 101:1–29. https://doi.org/10.1016/j.compositesa.2017.06.007

43. Kroisová D, Dvořáčková Š, Knap A, Knápek T (2023) Destruction of carbon and glass fibers during chip machining of composite systems. Polym 15(13):2888. https://doi.org/10.3390/polym15132888